Magnetic structure and effects of pressure on U_4PdGa_{12}

R. Jardin,[1] J.-C. Griveau,[1,*] K. Prokeš,[2] K. Gofryk,[1] A. V. Kolomiets,[3] P. Normile,[4] S. Heathman,[1] E. Colineau,[1] F. Wastin,[1] and J. Rebizant[1]

[1]*Institute for Transuranium Elements, Joint Research Center, European Commission, Postfach 2340, D-76125 Karlsruhe, Germany*

[2]*Helmholtz Centre Berlin, SF-2, Glienicker Strasse 100, Berlin 141 09, Germany*

[3]*Department of Physics, National University "Lvivska Polytechnica", 12 Bandera Street, 79013 Lviv, Ukraine*

[4]*Departamento de Física Aplicada, Universidad de Castilla–La Mancha, 13071 Ciudad Real, Spain*

(Received 13 November 2008; published 8 January 2009)

We report on the magnetic structure, thermopower, compressibility, and electrical resistivity under pressure of the recently discovered heavy-fermion antiferromagnet U_4PdGa_{12}. The ordering temperature of the annealed polycrystalline U_4PdGa_{12} is $T_N \sim 45.5$ K. The magnetic structure has been investigated by neutron diffraction. Extra reflections in the powder spectrum appear below ~46 K, in good agreement with macroscopic measurements. The simplest magnetic structure compatible with neutron-diffraction data is a collinear antiferromagnetic structure described by the propagation vector $\mathbf{q}=[001]$. In this case the ordered uranium moment amounts to $1.01(6)\mu_B$ and point along the a axis. Thermopower confirms the heavy-fermion features in this uranium intermetallic with positive and high values of Seebeck coefficient. The magnetic transition is clearly identified and induces an upturn below 45.5 K which is followed by a continuous decrease in $S(T)$ at lower temperature. Electrical resistivity measurements of U_4PdGa_{12} under pressure of up to 13.5 GPa indicate the disappearance of the magnetic ordering temperature T_N around $P_c=10$ GPa while compressibility measurements performed by x-ray diffraction up to 25 GPa do not show any structural phase transition related to this magnetic collapse. At higher pressure ($p>10$ GPa) and at low temperature, a non-Fermi-liquid behavior is observed, with a $T^{5/3}$ dependence of the resistivity. This suggests the possible occurrence of a quantum critical point near P_c.

DOI: 10.1103/PhysRevB.79.014409 PACS number(s): 74.25.Ha, 75.25.+z, 74.25.Fy, 74.62.Fj

I. INTRODUCTION

In the last decade, an interesting aspect of the physics of antiferromagnetic cerium and uranium compounds has been revealed. When pressure P is applied to compounds, such as $CeIn_3$,[1] $CePd_2Si_2$,[1,2] and UGa_3,[3] the Néel temperature T_N decreases and a quantum critical point (QCP) is reached at $P=P_c$ where $T_N \sim 0$. Additionally, superconductivity and/or non-Fermi-liquid (nFL) behaviors appear in the vicinity of P_c. These compounds present heavy-fermion features with a large electronic contribution γ_e to the specific heat C_p. This is one remarkable aspect of the recently reported heavy-fermion family of compounds An_4TGa_{12} (An=U, Np, and Pu; T=Fe, Co, Rh, and Pd).[4,5] All the studied compounds revealed an enhanced value of the Sommerfeld coefficient (with a maximum of 225 mJ/Pu mol^{-1} K^{-2} in Pu_4PdGa_{12}) but a clear magnetic phase transition occurs only in U_4PdGa_{12}. This material shows antiferromagnetic order evidenced by measurements of magnetization, specific heat, and electrical resistivity.[4] The An_4TGa_{12} compounds crystallize with a body-centered-cubic symmetry corresponding to the Y_4PdGa_{12} structure[6] (Fig. 1). This structure consists of $AnGa_3$ units of $AuCu_3$ cubic type into which 1/4 of the Ga octahedra are filled by a transition-metal atom. Therefore, gallium atoms leave the center of the faces of the actinoid cubes inducing a distortion and a shrinking of the empty octahedra together with a crystallographic superstructure with $a_{An_4TGa_{12}} \approx a'_{AnGa_3}$. Several aspects stress the interest in the study of U_4PdGa_{12}. This 4-1-12 structure is relatively close to the 1-4-12 skutterudite structure with formula MT_4X_{12}, where M is an electropositive cation, T is usually a transition metal, and X=P, As, or Sb. The most studied class among this family is based on rare earths and known for its strong electronic correlations but also because it presents unconventional superconductivity, such as $PrOs_4Sb_{12}$,[7] or the germanide systems RPt_4Ge_{12} (R=La, Pr, Sr, and Ba).[8] Unfortunately, actinoid-based skutterudite seem to be more difficult to produce and a few actinoid-based compounds have been reported with uranium[9] (UFe_4P_{12}), neptunium[10] ($NpFe_4P_{12}$), or thorium[11] ($ThPt_4Ge_{12}$) and only this last one presents superconductivity.

Another interesting aspect of U_4PdGa_{12} is that a large upturn in resistivity for $T<T_N$ is observed and could be re-

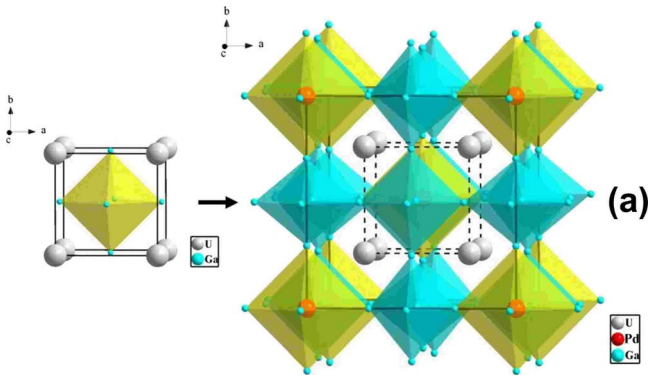

FIG. 1. (Color online) Projection on the (0 0 1) plane of the crystallographic structure of U_4PdGa_{12} (right) (Y_4PdGa_{12} type, $Im\bar{3}m$) derived from UGa_3 (left) by the partial filling of the gallium octahedra by a palladium atom and the doubling of the cell parameters.

lated to an opened gap induced by long-range magnetic order. This feature has already been reported for anisotropic systems such as UCu_5Al (Ref. 12), for instance; but U_4PdGa_{12} is *a priori* isotropic due to its cubic structure.

Therefore, we initiated different studies to determine or confirm the magnetic structure, the strong electronic correlations, and its stability versus different parameters. These results are discussed and compared to the properties of other related systems presenting magnetism collapse by external parameters (composition change or pressure effect).

II. CHARACTERIZATION AND EXPERIMENTAL DETAILS

A polycrystalline sample was prepared by arc melting the constituent elements in purified argon atmosphere on a water-cooled copper hearth, using a Ti-Zr alloy as oxygen getter. Starting materials were used in the form of commercial 3*N* Ga and palladium pieces and 3*N* pure uranium metal pieces. In order to ensure homogeneity, the arc-melted button was turned over and melted three times. Weight losses were smaller than 0.5%. It was then wrapped in tantalum foil, sealed in evacuated quartz tubes, annealed for 2 weeks at 800 °C, and quenched by submerging the quartz tubes into water. Samples extracted from this batch were characterized by x-ray powder-diffraction analysis and some small pieces suitable for single-crystal structure determination were mechanically extracted from this annealed button. These latter ones have been clearly identified as small single crystals as in Ref. 4. All analysis (powder and single crystals) confirm the structure of the material with the U_4PdGa_{12} stoichiometry. The majority of the original batch was ground in powder for neutron diffraction, while specific heat, thermopower, high-pressure resistivity, and compressibility measurements have been performed on samples extracted from the remaining batch.

Neutron-diffraction patterns were collected at few selected temperatures between 1.5 and 60 K using the multicounter flat-cone diffractometer E2 installed at the Berliner Neutron Scattering Center (BENSC) at the Helmholtz Center Berlin. The incident-neutron wavelength was 1.21 Å. For the temperature dependence study of the magnetic signal, we have utilized the double-axis diffractometer E4. In this case, the incident wavelength of 2.44 Å has been used. Two different standard Institut Laue-Langevin orange cryostats have been employed at the two instruments to achieve low temperatures. For these measurements, about 8 g of U_4PdGa_{12} was ground under inert atmosphere and encapsulated into a vanadium container with helium gas. The data were collected for 1.5 and 60 K and few selected intermediate temperatures and analyzed by means of the Rietveld profile procedure[13] using the program FULLPROF.[14] U magnetic form factor was taken from Ref. 15.

The thermoelectric power was measured from 6 to 300 K in a home-made setup on a sample presenting two polished faces extracted from the batch. Measurements were performed by setting a fixed gradient of temperature ΔT on the sample and by determining the voltage-induced ΔV using a nanovoltmeter (Keithley 2182). The value of the Seebeck coefficient $S=\frac{\Delta V}{\Delta T}$ of the sample is obtained after correction of the measured voltage by the calibration signal previously obtained on pure copper used as reference materials.

High-pressure resistivity measurements were performed on a small polycrystalline sample of typical dimensions $\sim 0.7\times 0.2\times 0.04$ mm^3 taken from the well-characterized ingot [the same used for the x-ray diffraction (XRD) experiment]. The sample was extracted from the batch under binoculars for the suitable shape. The electrical resistance was measured by a dc four-probe technique using constant current applied by a current source (Keithley 2124) and a nanovoltmeter (Keithley 2182). The sample and a thin foil of lead (manometer) were mounted in a pyrophyllite gasket and pressurized using steatite as pressure transmitter. Typical size of the pressure chamber was 1.5 mm for the pyrophyllite ring and 750 μm for the inner pressure room. The pressure change was performed at room temperature and the pressure cell was then cool down by nitrogen and helium. The pressure determination into the cell was achieved by determining the position of the superconducting transition of lead at low temperatures.[16] The gradient estimation was around 5% of the pressure measured by the lead: this represents up to 0.6 GPa at the maximum pressure achieved here ($\sim$14 GPa) and can be related to the width of superconducting transition of the manometer. The cell was made of nonmagnetic and good thermal conductor CuBe alloy and the anvils were made of pure WC.

For x-ray diffraction under pressure, a small powdered U_4PdGa_{12} sample was loaded into a Le Toullec–type (membrane) diamond-anvil cell [opening angle of 21° (2θ)] with beveled 300 μm diameter diamonds together with the pressure-transmitting medium (silicone oil) and the pressure gauge (single ruby ball of diameter <20 μm). Ruby was used to measure pressure by the fluorescence method. The pressure gradient is small in the full pressure range measured (<0.15 GPa). Stainless-steel gaskets of 150 μm (diameter) hole size and (indented) thickness 40 μm were used. All angle-dispersive XRD experiments were carried out using a Bruker rotating anode x-ray generator installed at ITU-Karlsruhe. X-ray wavelength and spot size (at the sample position) were 0.709 26 Å (Mo $K\alpha_1$) and 100×100 μm^2. Diffraction images were recorded with a Bruker SMART Apex charge-coupled device (CCD) (1024×1024 pixels of dimensions 61×61 μm^2). The images were then integrated using the ESRF FIT2D software,[17] which generates files for Rietveld refinement.

III. RESULTS

A. Neutron-diffraction experiment

The neutron-diffraction pattern recorded at 60 K, in the paramagnetic state of U_4PdGa_{12} revealed systematic extinction of reflections in agreement with the space group $Im\bar{3}m$ reported for this compound in literature.[6] Further refinements fully conform to the cubic Y_4PdGa_{12} type of structure. In this cubic body-centered structure (Fig. 1), eight magnetic U atoms occupy the 8(*c*) (1/4, 1/4, 1/4) Wyckoff position with the local symmetry $Im\bar{3}m$. There are furthermore two Pd atoms in the 2(*a*) (0, 0, 0) position, 12 Ga atoms in the 12(*d*)

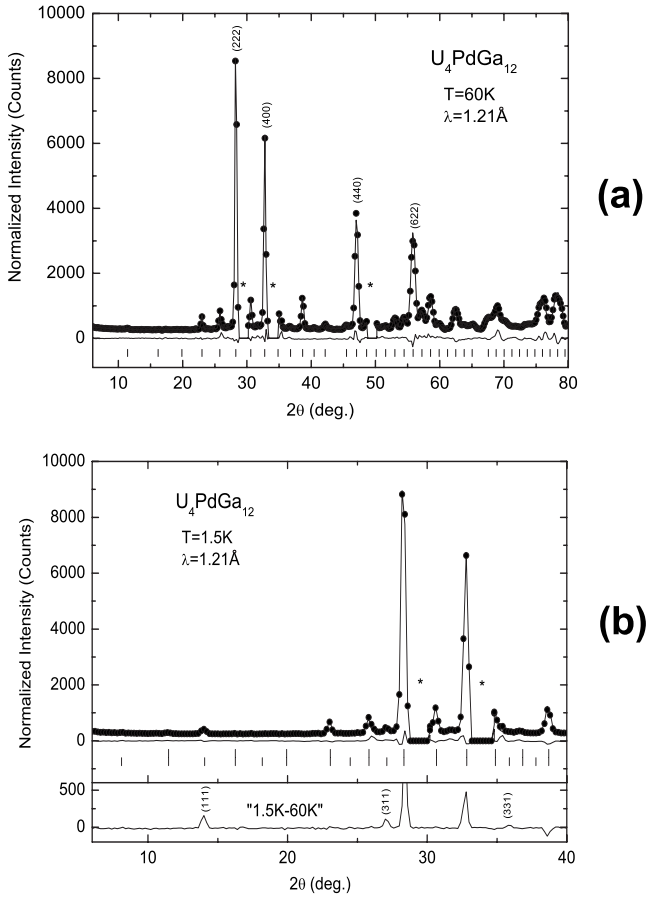

FIG. 2. The experimental (circles) diffraction pattern of U_4PdGa_{12} taken at (a) 60 K and (b) 1.5 K together with the best fit (full line through points) and the difference between them (line at the bottom). For the data taken at 1.5 K, only the low-angle portion is shown. Bragg reflection positions belonging to the magnetic (only at 1.5 K) and nuclear structure are marked at the bottom. The four strongest nuclear and the three most intense magnetic reflections are named. Stars denote regions excluded from the refinement because of substantial sample-environment contribution. For numerical results, see Table I.

(1/4, 0, 1/2) position, and another 12 Ga atoms in the 12(e) (x, 0, 0) position with the only free positional parameter $x \approx 0.29$. There are 2 f.u. in the cubic cell. Results of the best fit to data taken in the paramagnetic state of U_4PdGa_{12} at 60 K shown in Fig. 2(a) comprising of scale factor, cell parameters, one crystallographic-position parameter, background and peak-profile parameters, and isotropic thermal factor are summarized in Table I. Inclusion of the occupation parameters to the fit as free parameters did not improve the quality of the fit substantially. This suggests that our sample has stoichiometry close to the ideal 4:1:12 ratio.

As the temperature is lowered below the antiferromagnetic phase-transition temperature of 45 K, two clearly observable Bragg reflections that are forbidden for the parent paramagnetic space group appear, indicating that the symmetry of the magnetic structure is lower [Fig. 2(b)]. These reflections, which could be indexed with integer numbers as (111) and (311), respectively, are presumed to be solely due to magnetic order. No (100) reflection can be discerned. In

TABLE I. Structural and magnetic parameters of U_4PdGa_{12} determined above the magnetic phase transition (in the paramagnetic state) at 60 K and below the magnetic phase transition at 1.5 K using powder neutron diffraction.

Space group: $Im\bar{3}m$; $T=60$ K (paramagnetic)			
Atom	Site	Positional parameters	Occupation
U	8(c)	1/4,1/4,1/4	1.00 (fixed)
Pd	2(a)	0,0,0	0.96(2)
Ga	12(d)	1/4,0,1/2	0.99(1)
Ga	12(e)	0.2961(5),0,0	1.00(1)
Lattice constant $a=8.582(1)$ Å			
Agreement: $R_p=5.6\%$, $R_f=4.9\%$, $R_B=6.0\%$			
$T=1.5$ K			
Atom	Site	Positional parameters	Moment
U	8(c)	1/4,1/4,1/4	1.01(6)
Pd	2(a)	0,0,0	0
Ga	12(d)	1/4,0,1/2	0
Ga	12(e)	0.2948(5),0,0	0
Lattice constant $a=8.561(1)$ Å			
Agreement: $R_p=5.6\%$, $R_f=4.2\%$, $R_B=8.7\%$			

Fig. 3(a) we show the temperature dependence of the (111) Bragg reflection peak intensity. As can be seen, the antiferromagnetic phase transition of 45 K estimated from neutron data taken at the E2 instrument agrees relatively well with bulk measurements.

The detailed study has been performed on the double-axis E4 diffractometer. The temperature dependence of the (111) Bragg reflection peak intensity as measured at E4 is shown in Fig. 3(b) together with fits to a phenomenological dependence of the form $I=I_0(1-\frac{T}{T_N})^{2\beta}$, with β as the critical exponent.

This function was developed to describe the data in a critical region close to the phase transition and gives indeed a rather good description of the data. The best fit yields $I_0=222.2\pm13.9$ counts, $T_N=46.6\pm1.2$ K, and $\beta=0.25\pm0.06$ for fit to data above 38 K. As can be seen, the fitted β value is relatively close to 0.31 expected for the three-dimensional (3D) Ising model. The small difference observed for T_N in this part of experiment can be caused by, e.g., a temperature gradient in the cryostat (the thermometry has to be at a certain distance from the sample because of irradiation by neutrons), not ideal thermal contact between powder grains or by short-range order in the vicinity of T_N.

Both extra reflections that appear below T_N can be indexed either with propagation vector $\boldsymbol{q}_1=(0\ 0\ 0)$ or $\boldsymbol{q}_2=(0\ 0\ 1)$. In both cases it follows that the magnetic unit cell has the same size as the crystallographic one. The possible mutual orientations of magnetic moments within each crystallographic cell were derived for both propagation vector models with the help of computer code MODY (Ref. 18) that utilizes space-group symmetry.[19] There are four irreducible

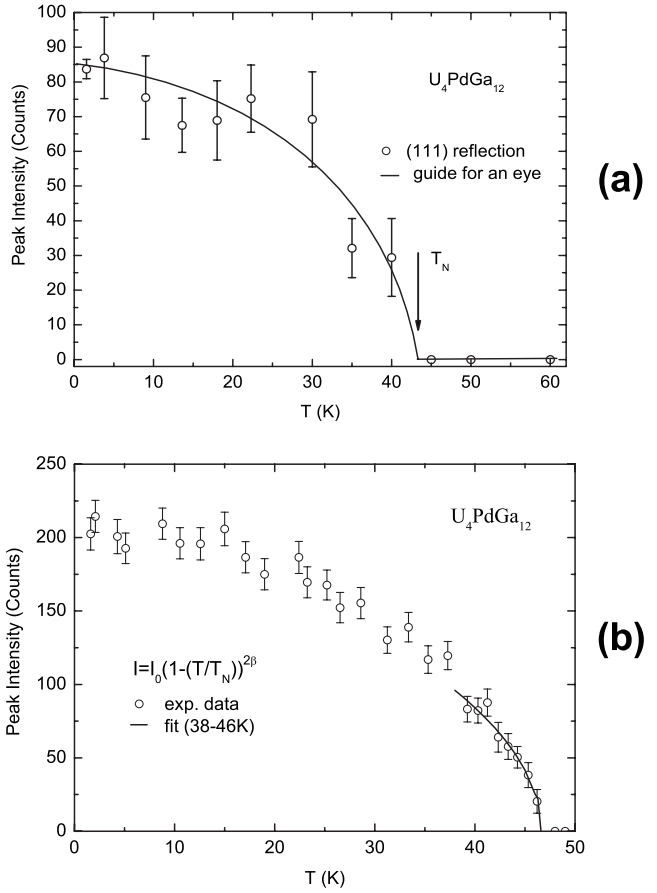

FIG. 3. Neutron-diffraction measurements: temperature dependence of (111) Bragg reflections intensity originating from magnetic order in U_4PdGa_{12} as measured on the (a) E2 diffractometer and the (b) E4 diffractometer. In (a), the full line represents a guide for the eyes; whereas in (b), the full line represents the best fit to the mean-field-type dependence for data above 38 K.

representations for each possible propagation vector that are one, two, or three dimensional. Basically, magnetic structures with all three crystallographic components are allowed. Magnetic structure models for the two propagation vectors $\boldsymbol{q}_1$ and $\boldsymbol{q}_2$ that follow from the analysis differ only in one respect. Among $\boldsymbol{q}_1=(0\ 0\ 0)$ models there is no magnetic structure that would be collinear antiferromagnetic and among those belonging to $\boldsymbol{q}_2=(0\ 0\ 1)$ there is no collinear ferromagnetic structure allowed.

Unfortunately, the nature of the present neutron-diffraction experiment does not allow the determination of the U moment directions from principal reasons. Any collinear allowed orientation among others also along one of the principal axes, along one of the face diagonals, or along the body diagonal lead to identical diffraction patterns and agreement with experimental data. This question can be answered merely in a single-crystal experiment with some external perturbation. In Fig. 4 we show the simplest magnetic structure of U_4PdGa_{12} (supposing the moments along one of the principal axes) that is in accord with experimental data. The structure is antiferromagnetic and consists of equal-size U moments of $1.01 \pm 0.06 \mu_B$. Four of them, in positions (1) $\frac{1}{4},\frac{1}{4},\frac{1}{4}$; (2) $\frac{1}{4},\frac{3}{4},\frac{3}{4}$; (3) $\frac{3}{4},\frac{1}{4},\frac{3}{4}$; and (4) $\frac{3}{4},\frac{3}{4},\frac{1}{4}$ on one side and

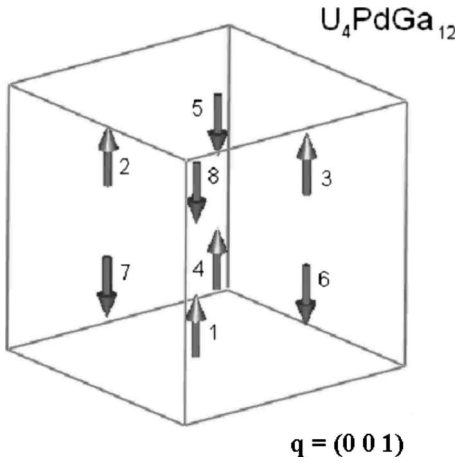

FIG. 4. Schematic representation of the simplest antiferromagnetic structure of U_4PdGa_{12} that is in accord with experimental data taken at low temperatures. Only U magnetic moments are shown. Moments are of equal size of $1.01(6)\mu_B$. Although in the picture shown to point along one of the equivalent principal axis, on the basis of powder experiment one cannot conclude whether they align indeed along the principal axis along the face diagonal or along the body diagonal.

those at (5) $\frac{3}{4},\frac{3}{4},\frac{3}{4}$; (6) $\frac{3}{4},\frac{1}{4},\frac{1}{4}$; (7) $\frac{1}{4},\frac{3}{4},\frac{1}{4}$; and (8) $\frac{1}{4},\frac{1}{4},\frac{3}{4}$ on the other are oriented antiparallel with respect to each other. The best fit to experimental data taken at 1.5 K for the above-mentioned magnetic structure is shown in Fig. 2(b) and the numerical results are given in Table I.

B. Thermoelectric power

The Seebeck coefficient is a sensitive probe of the electronic band structure close to the Fermi level.[20] Thus, the thermoelectric power measurement could reveal important information about the band structure in the vicinity of the Fermi energy. The temperature dependence of the Seebeck coefficient of U_4PdGa_{12} is displayed in Fig. 5. At room temperature the thermopower has a positive value of about

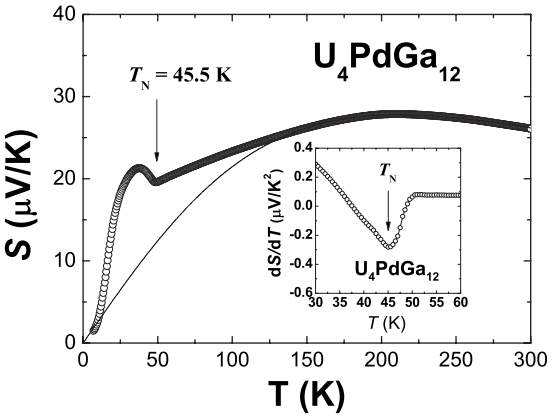

FIG. 5. Temperature dependence of the Seebeck coefficient of U_4PdGa_{12}. The solid line is a fit of Eq. (2) to the experimental data. Inset: the derivative of the thermopower in the vicinity of the magnetic phase transition. Arrows point to the position of T_N.

26 μV/K. This value is 1 order of magnitude larger than the one in simple metals. With decreasing temperature, the Seebeck coefficient slightly increases and forms a broad maximum around 200 K. Similarly to the electrical resistivity, just below the magnetic phase transition the Seebeck coefficient increases and then the $S(T)$ curve exhibits a distinct hump with a maximum at 35 K.

In general, the magnitude and the overall temperature dependence of the thermopower of U_4PdGa_{12} closely resembles that found for uranium-based heavy-fermion compounds [e.g., UPt_2In (Ref. 20) and UPd_2Sb (Ref. 21)]. To describe the temperature variations in the Seebeck coefficient in these systems a simple phenomenological model was used.[22] It takes into account scattering processes of conduction electrons by a narrow $5f$ quasiparticle band. Assuming the band to have a Lorenzian form,

$$n(E) = \frac{\Gamma}{\varepsilon^2 + \Gamma^2} \tag{1}$$

where Γ denotes its width and ε is its position in respect to the Fermi energy. The $S(T)$ variation may be expressed by a modified Mott formula:[20,22]

$$S(T) = \frac{2\pi^2 k_B^2}{3|e|} \frac{\varepsilon T}{\pi^2 T^2 k_B^2/3 + \varepsilon^2 + \Gamma^2}. \tag{2}$$

As shown in Fig. 5 it provides also a quite good approximation of the thermoelectric power of U_4PdGa_{12} above 120 K. The least-squares fit of Eq. (2) to the experimental data yielded the parameters $\varepsilon = 6$ meV and $\Gamma = 33$ meV, which are similar to those derived for $5f$-electron-based compounds with strong electronic correlations.[20,21]

C. Resistivity under pressure

Electrical resistivity of U_4PdGa_{12} was studied on two pieces of the annealed polycrystalline sample. The pressure was subsequently gradually increased up to 13.5 GPa and at each pressure the resistance was measured in the temperature range 1.3–300 K. Figure 6 shows the temperature dependence of R/R_{300} at several pressures. At ambient pressure the resistance value decreases slightly with temperature down to 52 K, where an upturn is observed, suggesting the opening of a magnetic gap as for UCu_5Al.[23] Then, we observe a clear increase in the resistivity when cooling down below T_N. A change in slope around 45 K is identified as corresponding to the Néel temperature. These results at low pressure are very similar to ambient pressure measurement[4] confirming the homogeneity of the material.

Increasing pressure on U_4PdGa_{12} results in three main consequences on the electrical resistivity. The first one is that we observe a tendency to a "metallic" character of the resistivity: U_4PdGa_{12} shows a continuous decrease in the resistivity with increasing pressure. The upturn is less and less pronounced and transport curves present a positive curvature dominating the whole temperature range above the magnetic collapse. This curvature could be associated to spin-fluctuations scattering features as the amplitude of the magnetic gap decreases progressively. The second effect is that

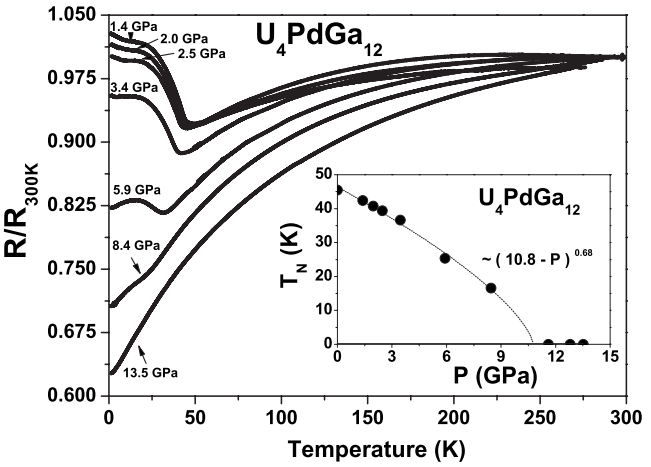

FIG. 6. Temperature dependence of the normalized electrical resistance $[R(T)/R_{300K}]$ of U_4PdGa_{12} at selected pressures. We observe a clear disappearance of the magnetic upturn below T_N. The inset presents the $T_N(p)$ diagram obtained using the derivative of resistivity to determine the position of T_N. The best fit of $T_N(p)$ by $\sim|P-P_c|^n$ relation is obtained for the critical exponent $n=0.68 \sim 2/3$.

the Néel temperature also decreases with increasing pressure and vanishes in the 10 GPa range (Fig. 6). This could be explained by the disappearance of the associated moments or by the destruction of the long-range magnetic order at this critical pressure. Magnetization or neutron diffraction at low pressure would be of great interest even only in the 1–3 GPa range to estimate the variation in value of the magnetic moment with pressure and confirmed one of these scenarios. The variation in the Néel temperature as a function of pressure is shown in the inset of Fig. 6 and can be fitted by the law $T_N \approx |P-P_c|^n$ with estimated critical pressure $P_c \sim 10.8$ GPa and a critical exponent $n \sim 0.68$. This exponent value is very close to 2/3 that is expected for a 3D spin-fluctuations regime in the case of magnetic collapse.[24–26] This result confirms our description of U_4PdGa_{12} as an isotropic magnetic system and is compatible with the magnetic structure hypothesis deduced from neutrons measurements. Finally, the third aspect is that in the pressure range $11.3 < P < 13.5$ GPa, the low-temperature electronic resistivity exhibits a $T^{5/3}$ dependence for $T < 5$ K characteristic of a non-Fermi-liquid behavior. Several electrical resistance curves are presented in Fig. 7. This 5/3 exponent is usually related to 3D ferromagnetic fluctuations.[27] At low pressure, the shape of the resistivity presents a clear upturn for $T < T_N$. It is only when the high magnetic contribution to resistivity is reduced (destroyed) by pressure that the small electronic contribution to resistivity can be observed. The question remains of the existence of this nFL regime just before the collapse of magnetic order or if this $T^{5/3}$ regime is directly induced by the reduction in the magnetic gap. Moreover we do not know if the nFL remains at higher pressure ($P > 14$ GPa). Nevertheless at 13.5 GPa, we do not observe any Fermi-liquid (FL) behavior ($R \approx T^2$). It was then important to examine the possible link of the magnetic collapse of T_N around 10 GPa to a possible crystallographic phase-transition compression.

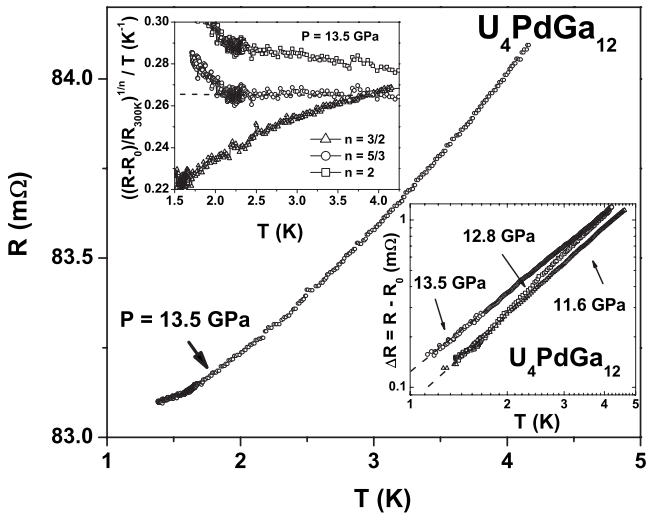

FIG. 7. Resistance of annealed polycrystalline sample of U_4PdGa_{12} at 13.5 GPa. To determine the T dependence at low temperature, we achieved exponent treatment, plotting $(R\text{-}R_0)^{1/n}/T$, and using $n=3/2$, 5/3, and 2 (top left inset). R_0 corresponds to the residual resistance extrapolation. The constant behavior is observed only for $n=5/3$ in this temperature range confirming the $T^{5/3}$ behavior of the resistance. The validity of the nFL regime is presented for the three pressures measured above T_N collapse (11.6, 12.8, and 13.5 GPa) by plotting in log-log scale $\Delta R=R\text{-}R_0$ vs T (bottom right inset). The dashed lines are guides for the eyes.

D. X-ray diffraction under pressure

Using the diamond-anvil cell, the sample was studied up to ~25 GPa. Some x-ray-diffraction patterns of U_4PdGa_{12} at high pressure are shown in Fig. 8. They can be indexed according to the Y_4PdGa_{12}-type structure, which was conserved throughout the entire pressure range. The recording of seven diffraction lines persisting up to 25 GPa allows us to derive the compressibility at room temperature. The relative volume versus pressure relation of U_4PdGa_{12} is plotted in the inset of Fig. 8. There is no anomalous volume contraction. The small bump observed around 6 GPa is assumed to be due to the freezing of the silicone-oil transmitting medium.[28] By fitting the volume-pressure data with the Birch-Murnaghan equation,[29,30]

$$P=\frac{3}{2}B_0\left[\left(\frac{V}{V_0}\right)^{-7/3}-\left(\frac{V}{V_0}\right)^{-5/3}\right]\times\left[1-\frac{3}{4}(4-B_0')\left[\left(\frac{V}{V_0}\right)^{-2/3}-1\right]\right], \quad (3)$$

the bulk modulus B_0 and its pressure derivative B_0' were obtained.

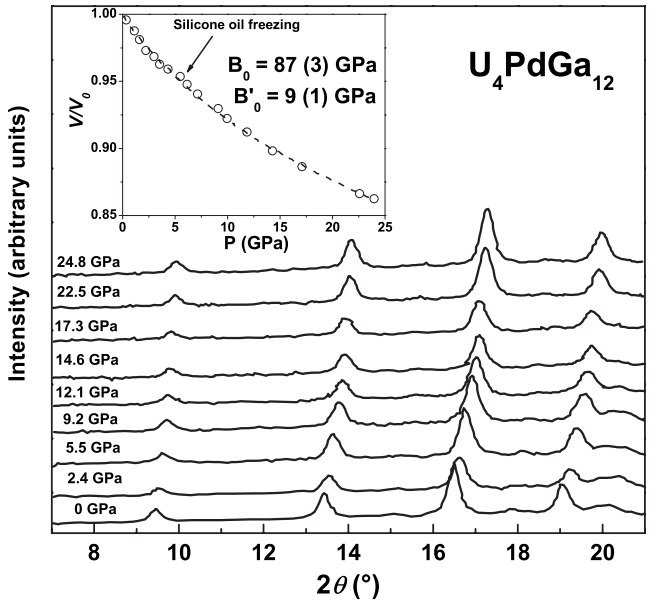

FIG. 8. X-ray-diffraction patterns and relative volume (inset) of U_4PdGa_{12} at high pressure. In the inset, the dashed line represents the fitting with the Birch-Murnaghan equation with parameters given in Table II.

TABLE II. Crystallographic and volume parameters in U_4PdGa_{12}, UGa_3, and $NpGa_3$.

Compound	$d_{An\text{-}An}$ (Å)	δ_{calc} (g/cm^3)	Structure	B_0 (GPa)	B_0'	Reference
U_4PdGa_{12}	4.297	9.92	Y_4PdGa_{12}	87(3)	9(1)	ITU
UGa_3	4.261	9.60	$AuCu_3$	90(2)	5(1)	23
$NpGa_3$	4.246	9.68	$AuCu_3$	75(2)	6(2)	24

As there is no other work to our knowledge on U_4MGa_{12} (M=transition metal), we compare our results to those obtained for UGa_3 (Ref. 31) and $NpGa_3$ (Ref. 32) polycrystalline samples (see Table II). As mentioned in Sec. I, the Y_4PdGa_{12} structure (U_4PdGa_{12}) can be regarded as the result of partially filling the octahedral voids of gallium atoms in the cubic-close-packed $AuCu_3$ structure (UGa_3 and $NpGa_3$). The calculated values of the bulk modulus are essentially inversely proportional to the lattice constant, which amounts to saying that the compressibility is proportional to the lattice constant. But in the case of U_4PdGa_{12}, we should take into account the partial filling of the gallium octahedra and therefore we should not only think about the An-An distance but also about the calculated density. According to the theory, for analog compounds, the bulk modulus decreases as the atomic number increases.[33]

IV. DISCUSSION

Recently we reported on a family of heavy-fermion materials U_4TGa_{12} (T=Fe, Co, Rh, and Pd).[4] Among these four compounds only U_4PdGa_{12} exhibits magnetic order; therefore we selected this Pd-based compound for further investigations by neutron diffraction, thermopower, high-pressure electrical resistivity, and x-ray diffraction. The crystal structure of U_4PdGa_{12} derives from the well-known $AuCu_3$ type adopted by UGa_3. Our physical investigations show that strong analogies can be also drawn between U_4PdGa_{12} and UGa_3. They might be both collinear antiferromagnets, with moments parallel to the propagation vector. While the q vectors are different ((0 0 1) and $(\frac{1}{2},\frac{1}{2},\frac{1}{2})$ for U_4PdGa_{12} and

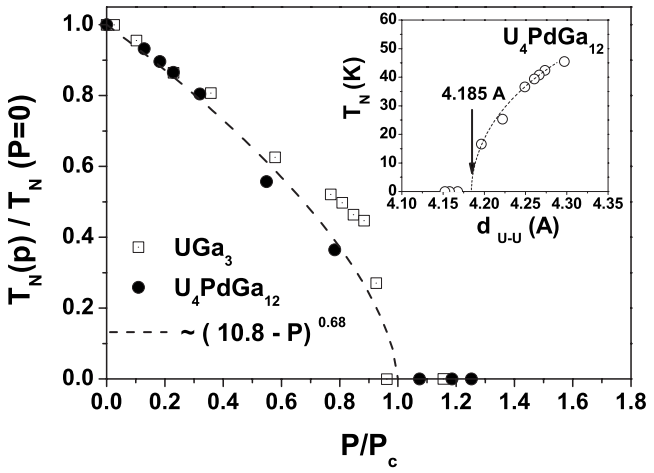

FIG. 9. Normalized $T_N(P)$ curves for U_4PdGa_{12} (circles) and UGa_3 (squares). The inset shows the evolution of ordering temperature T_N versus the uranium-uranium atomic distance in the cell.

UGa_3, respectively), other magnetic parameters are relatively close such as the magnitude of the Néel temperature (45.5 and 64 K, respectively) and magnetic moments (1.01 and 0.74 μ_B, respectively).[34] X-ray-diffraction experiments under pressure show that no crystallographic phase transition occurs up to 25 GPa, such as in UX_3 (X=Al, Si, Ga, Ge, In, and Sn) and $NpGa_3$. Moreover, the calculated bulk modulus of U_4PdGa_{12} is very close to the one of UGa_3 and $NpGa_3$ (see Table II), which means that inserting transition-metal atoms in some of the gallium octahedra does not drastically affect the compressibility of the material. On the other side, the electrical resistivity experiments under pressure show that the Néel temperature decreases steeply with increasing pressure until the magnetic collapse at $\approx$10 GPa. It is worth noting that in UGa_3, the same phenomenon occurs with T_N =67 K and P_c=2.6 GPa.[3] From these results, it is possible to extract the critical uranium-uranium distance d(U-U)$_c$. For the binary compound UGa_3, d(U-U)$_c$ amounts to 4.23 Å (which corresponds to $V/V_0 \approx 97.8\%$), whereas for U_4PdGa_{12}, d(U-U)$_c$ is 4.18 Å ($V/V_0 \approx 92.7\%$) (inset of Fig. 9). This value is largely above the Hill limit ($r_{\mathrm{Hill}} \approx 3.5$ Å) and the d(U-U) distance does not seem to control magnetism aspect alone. This means that Pd atoms play probably an effective role in the magnetism of U_4PdGa_{12}.

The binary uranium intermetallic compounds UX_3 (where X is an element of group IIIB or IVB of the Periodic Table) with the cubic $AuCu_3$-type structure, exhibit a large variety of magnetic properties including Pauli paramagnetism (USi_3 and UGe_3), spin fluctuations (USn_3 and UAl_3), and antiferromagnetism (UPb_3, UIn_3, and UTl_3).[35] A pressure phase diagram of the antiferromagnet UIn_3 has been constructed from the electrical resistivity measurements up to 9 GPa. T_N increases monotonically with increasing pressure from 88 K at ambient pressure up to 127 K at 9 GPa.[36] Recently, the pressure dependence of the antiferromagnetic transition temperature T_N has also been studied for UPb_3 by electrical resistivity. It was found that T_N first increases with increasing pressure from 28 K to a maximum value of 38 K at 5 GPa then decreases with increasing pressure. The maximum pressure of 8 GPa was not enough to suppress the antiferromagnetic ordering and they estimated the critical pressure to be around 10 GPa.[37] Therefore, no systematic behavior of the Néel temperature under pressure can be predicted for all antiferromagnetic UX_3 compounds, which highlights the analogy between UGa_3 and U_4PdGa_{12}. Indeed, the normalized $T_N(P)$ curves for U_4PdGa_{12} and UGa_3 (data taken from Ref. 3) superpose rather well. Interestingly, considering doped systems, such as $U(Ga_{1-x}Sn_x)_3$ or $U(Ga_{1-x}Ge_x)_3$ systems,[38,39] we observe a similar behavior of the resistivity of U_4PdGa_{12} presenting an upturn at the ordering temperature T_N and more specifically for some concentration of Ge ($0.05 < x < 0.15$). Substituting gallium by germanium into the matrix induces a collapse of the magnetic order and the disappearance of this upturn (x=0.2).[39] In this case, we could consider that for some concentrations germanium plays the same role as a positive pressure effect on U_4PdGa_{12}.

Another common feature between these two compounds concerns the nFL behavior in the low-temperature part of the resistivity observed around the critical pressure. As mentioned in Ref. 3, the electrical resistivity at ambient pressure of UGa_3 follows a T^2 dependence (FL) below about 20 K. This feature was confirmed by Aoki *et al.*[40] that also showed a non-Fermi-liquid behavior in the critical pressure region and return to a FL regime above 5 GPa. As explained before, the resistivity shape of U_4PdGa_{12} prevents us to observe a FL regime for pressure below P_c. Nevertheless, for $P_c < P < 13.5$ GPa, a $T^{5/3}$ dependence of the resistivity indicates a nFL regime which still exists at the maximum pressure of our study P=13.5 GPa. The observation of a nFL state together with the collapse of the Néel temperature suggest the possible occurrence of a magnetic QCP, similar to that observed in UGa_3 single crystals[3] and in $U(Ga_{1-x}Ge_x)_3$.[41] In such conditions, superconductivity may appear, as discussed for $CePd_2Si_2$ (Ref. 42) and $CeCu_2Ge_2$.[43] However, no hint of superconductivity has been observed in U_4PdGa_{12} up to 13.5 GPa and down to 1.3 K.

V. CONCLUSION

Annealed polycrystalline samples of U_4PdGa_{12} have been characterized by x-ray diffraction and measured by neutron diffraction, thermopower, electrical resistivity under pressure, and x-ray diffraction under pressure. Our neutron-scattering study of the moderate heavy-fermion U_4PdGa_{12} confirms the antiferromagnetic phase transition occurring at $T_N \approx 45$ K and the crystallization in the Y_4PdGa_{12} structure. The simplest model used to interpret extra reflections in the powder spectrum below T_N is the collinear antiferromagnetic structure with the propagation vector $\mathbf{q}$=[001]. In this case, the ordered uranium moment amounts to $1.01(6)\mu_B$ and points along the a axis. More complicated magnetic structures cannot be excluded since we used a powder sample and the symmetry of the phase is cubic. The temperature variation in the Seebeck coefficient for U_4PdGa_{12} is typical for systems with strong hybridization of $5f$ electrons with conduction band. It confirms the heavy-fermion aspects with enhancement of effective masses of carriers that was previously reported by ambient pressure measurements, especially specific-heat studies at low temperatures[4] and reinforcing

analogy with actinoid-based skutterudite systems presenting strong electronic correlations. A magnetic collapse is revealed by electrical resistivity measurements under pressure and occurs around $P_c = 10$ GPa. This phenomenon associated to the nFL behavior observed for pressures close to P_c points to the possible existence of a QCP. Moreover no crystallographic phase transition occurs up to 25 GPa, as shown by x-ray diffraction but the magnetic collapse is achieved before the Hill limit ($d_{\text{U-U}} \sim 4.18$ Å > 3.5 Å). This aspect and the strong analogies to UGa_3 exhibiting QCP stress the importance of Pd as a transition metal in U_4PdGa_{12} for magnetic properties. All measurements indicate that U_4PdGa_{12} is an antiferromagnet at 45 K which agrees quite well with previous study.[4] The small difference with reported data may be related to the thermal gradient induced by the measurements process, the way of the determination of T_N, as well as to the annealing process. Neutron measurements under pressure or complementary work on single crystals especially at the QCP at very low temperature ($T < 1$ K) will be of great importance to help in the understanding of this uranium-based representative of the Y_4PdGa_{12} family.

ACKNOWLEDGMENTS

R.J., A.K., P.N., and K.G. acknowledge the European Commission for support in the frame of the "Training and Mobility of Researchers" program. The authors are very grateful to R. Caciuffo and T. Gouder for their remarks and careful reading.

*jean-christophe.griveau@ec.europa.eu

[1] N. D. Mathur, F. M. Grosche, S. R. Julian, I. R. Walker, D. M. Freye, R. K. W. Haselwimmer, and G. G. Lonzarich, Nature (London) **394**, 39 (1998).
[2] N. Kernavanois, S. Raymond, E. Ressouche, B. Grenier, J. Flouquet, and P. Lejay, Phys. Rev. B **71**, 064404 (2005).
[3] M. Nakashima, Y. Haga, F. Honda, T. Eto, G. Oomi, T. Kagayama, N. Takeshita, T. Nakanishi, N. Mori, S. Aoki, R. Settai, and Y. Onuki, J. Phys.: Condens. Matter **13**, L569 (2001).
[4] R. Jardin, E. Colineau, J. C. Griveau, P. Boulet, F. Wastin, and J. Rebizant, J. Alloys Compd. **432**, 39 (2007).
[5] R. Jardin, E. Colineau, F. Wastin, J. Rebizant, and J.-P. Sanchez, Physica B **378–380**, 1031 (2006).
[6] L. O. Vasilenko, A. S. Noga, Yu N. Grin, M. D. Koterlin, and Ya P. Yarmolyuk, Izv. Akad. Nauk. SSSR, Met. **5**, 216 (1988).
[7] E. D. Bauer, N. A. Frederick, P. C. Ho, V. S. Zapf, and M. B. Maple, Phys. Rev. B **65**, 100506(R) (2002).
[8] R. Gumeniuk, W. Schnelle, H. Rosner, M. Nicklas, A. Leithe-Jasper, and Yu. Grin, Phys. Rev. Lett. **100**, 017002 (2008).
[9] G. P. Meisner, M. S. Torikachvili, K. N. Yang, M. B. Maple, and R. P. Guertin, J. Appl. Phys. **57**, 3073 (1985).
[10] D. Aoki, Y. Haga, Y. Homma, H. Sakai, S. Ikeda, Y. Shiokawa, E. Yamamoto, A. Nakamura, and Y. Onuki, J. Phys. Soc. Jpn. **75**, 073703 (2006).
[11] D. Kaczorowski and V. H. Tran, Phys. Rev. B **77**, 180504(R) (2008).
[12] V. H. Tran, R. Tróc, J. Stepien-Damm, T. Komatsubara, F. Steglich, R. Hauser, and E. Bauer, Phys. Rev. B **66**, 054421 (2002).
[13] H. M. Rietveld, J. Appl. Crystallogr. **2**, 65 (1969).
[14] T. Roisnel and J. Rodríguez-Carvajal, Mater. Sci. Forum **378**, 118 (2001).
[15] A. J. Freeman, J. P. Desclaux, G. H. Lander, and J. Faber, Jr., Phys. Rev. B **13**, 1168 (1976).
[16] B. Bireckhoven and J. Wittig, J. Phys. E **21**, 841 (1988).
[17] A. P. Hammersley, S. O. Svensson, M. Hanfland, A. N. Fitch, and D. Haüsermann, High Press. Res. **14**, 235 (1996).
[18] W. Sikora, F. Bialas, L. Pytlik and J. Malinowski, computer code MODY for WINDOWS, version 6.IV.2004, 2004.
[19] E. F. Bertaut, Acta Crystallogr., Sect. A: Cryst. Phys., Diffr., Theor. Gen. Crystallogr. **24**, 217 (1968).
[20] Y. Bando, T. Suemitsu, K. Takagi, H. Tokushima, Y. Echizen, K. Katoh, K. Umeo, Y. Maeda, and T. Takabatake, J. Alloys Compd. **313**, 1 (2000).
[21] K. Gofryk, D. Kaczorowski, and A. Czopnik, Solid State Commun. **133**, 625 (2005).
[22] U. Gottwick, K. Gloss, S. Horn, F. Steglich, and N. Grewe, J. Magn. Magn. Mater. **47–48**, 536 (1985).
[23] V. H. Tran, J. C. Griveau, R. Troć, J. Rebizant, and F. Wastin, J. Magn. Magn. Mater. **272–276**, E61 (2004).
[24] A. J. Millis, Phys. Rev. B **48**, 7183 (1993).
[25] T. Moriya and T. Takimoto, J. Phys. Soc. Jpn. **64**, 960 (1995).
[26] M. A. Continentino, Phys. Rev. B **57**, 5966 (1998).
[27] G. G. Lonzarich, in *The Electron*, edited by M. Springford (Cambridge University Press, Cambridge, 1997), Chap. 6.
[28] L. Gerward, J. Staun Olsen, U. Benedict, H. C. Abraham, and F. Hulliger, High Press. Res. **13**, 327 (1995).
[29] F. Birch, Phys. Rev. **71**, 809 (1947).
[30] F. D. Murnaghan, Am. J. Math. **59**, 235 (1937).
[31] T. Le Bihan, S. Heathman, S. Darracq, C. Abraham, J. M. Winand, and U. Benedict, High Temp. - High Press. **27–28**, 157 (1995/1996).
[32] S. Zwirner, V. Ichas, D. Braithwaite, J. C. Waerenborgh, S. Heathman, W. Potzel, G. M. Kalvius, J. C. Spirlet, and J. Rebizant, Phys. Rev. B **54**, 12283 (1996).
[33] M. S. S. Brooks, B. Johansson, and H. L. Skriver, in *Handbook on the Physics and Chemistry of the Actinides*, edited by A. J. Freeman and G. H. Lander (Elsevier, Amsterdam, 1984), Vol. 1, p. 153.
[34] P. Dervenagas, D. Kaczorowski, F. Bourdarot, P. Burlet, A. Czopnik, and G. H. Lander, Physica B **269**, 368 (1999).
[35] D. D. Koelling, B. D. Dunlap, and G. W. Crabtree, Phys. Rev. B **31**, 4966 (1985).
[36] Y. Haga, F. Honda, T. Eto, G. Oomi, T. Kagayama, N. Takeshita, N. Mori, T. Nakanishi, Y. Tokiwa, D. Aoki, and Y. Onuki, J. Phys. Soc. Jpn. **71**, 2019 (2002).
[37] Y. Haga, E. Yamamoto, Y. Onuki, M. Nakashima, D. Aoki, Y. Onuki, M. Hedo, and Y. Uwatoko, Acta Phys. Pol. B **34**, 1239 (2003).
[38] D. Kaczorowski, R. Tróc, D. Badurski, A. Böhm, L. Shlyk, and F. Steglich, Phys. Rev. B **48**, 16425 (1993).

[39] D. Kaczorowski, R. Hauser, and A. Czopnik, Physica B **230–232**, 35 (1997).

[40] D. Aoki, N. Suzuki, K. Miyake, Y. Inada, R. Settai, K. Sugiyama, E. Yamamoto, Y. Haga, Y. Onuki, T. Inoue, K. Kindo, H. Sugawara, H. Sato, and H. Yamagami, J. Phys. Soc. Jpn. **70**, 538 (2001).

[41] K. Gofryk and D. Kaczorowski, Acta Phys. Pol. B **34**, 1213 (2003).

[42] F. M. Grosche, S. R. Julian, N. D. Mathur, and G. G. Lonzarich, Physica B **223 & 224**, 50 (1996).

[43] D. Jaccard, P. Link, E. Vargoz, and K. Alami-Yadri, Physica B **230–232**, 297 (1997).